LIMNOLOGY
and
OCEANOGRAPHY

ASLO

Limnol. Oceanogr

doi: 10.1002/lno.10953

Effect of hydrological variability on the biogeochemistry of estuaries across a regional climatic gradient

Paul A. Montagna,[1*] **Xinping Hu**,[2] **Terence A. Palmer**,[1] **Michael Wetz**[3]

[1]Harte Research Institute for Gulf of Mexico Studies, Texas A&M University-Corpus Christi, Corpus Christi, Texas
[2]Department of Physical and Environmental Sciences, Texas A&M University-Corpus Christi, Corpus Christi, Texas
[3]Department of Life Sciences, Texas A&M University-Corpus Christi, Corpus Christi, Texas

Abstract

Given projected changes in river flow to coastal regions worldwide due to climate change and increasing human freshwater demands, it is necessary to determine the role hydrology plays in regulating the biogeochemistry of estuaries. A climatic gradient exists along the Texas coast where freshwater inflow balance ranges from hydrologically positive to negative (where evaporation exceeds inflow) within a narrow latitudinal band, providing a natural experiment for examining inflow effects. Four Texas estuaries ranging from mesosaline to hypersaline were studied for 3 yr to determine how hydrological changes alter the biogeochemistry within and among the estuaries. Trends in dissolved inorganic nutrients, chlorophyll, dissolved organic matter, and carbonate chemistry indicated that these estuaries had drastically different biogeochemical signatures. Nutrients and chlorophyll patterns illustrated an emerging paradigm where phytoplankton biomass in positive estuaries is supported by "new" nitrogen from riverine input, while high concentrations of reduced nitrogen (organic, ammonium) allowed for high chlorophyll in the negative estuary. For carbonate chemistry, a positive estuary receiving river input from a limestone-dominated watershed was well-buffered under moderate to high freshwater inflow conditions. When weathering products were diluted during high-flow conditions, there is carbonate undersaturation (for aragonite) and decreases in pH. However, "acidification" was not observed in the negative estuary because evaporation concentrated the dissolved species and increased buffering capacity. Hydrological changes over spatial gradients are analogous to climatic changes over time, meaning climate change forecasts of higher temperatures and decreased precipitation can make the biogeochemistry of fresher estuaries change to the patterns of saltier estuaries.

Estuaries are coastal indentations where freshwater mixes with seawater (Pritchard 1967), and are found everywhere in the world. However, the characteristics of the coasts can vary dramatically in terms of the geological setting, climate regime, and tidal regime. These three characteristics drive differences in geomorphology, hydrology, and physical exchange, and the interaction among these drivers will result in different estuary conditions everywhere. The vast number of combinations of these three drivers has led some to posit that there is an "estuarine signature" that is unique to each estuary (Turner 2001; Montagna et al. 2013).

The hydrology of an area controls water balance in an estuary, which is the sum of water sources minus the sum of water losses. The sources of freshwater to the coastal zone include: rivers, streams, groundwater, direct precipitation, point-source discharges, and non-point-source runoff. There are fewer mechanisms that cause losses of freshwater, but these primarily include evaporation and freshwater diversions for human use. There are three classes of estuaries based on natural hydrological processes: (1) positive estuaries where freshwater input exceeds evaporation; (2) neutral estuaries where the sources and sinks are in balance; and (3) negative or inverse estuaries where evaporation exceeds the combined sources of freshwater (Pritchard 1952; Potter et al. 2010). Many estuaries in the world have strong year-to-year hydrological variability caused by climatic variability.

The Texas coast located in the northwestern Gulf of Mexico provides a unique opportunity to examine questions about the role of hydrology in determining an estuarine signature. There are seven major estuarine systems along the 600 km of coastline, and all have similar geomorphic structure and physiography (Longley 1994; Montagna et al. 2013). The estuaries are lagoons with barrier islands parallel to the mainland. The lagoon opens to a large primary bay, and there is a constriction between the primary bay and the smaller secondary bay.

*Correspondence: paul.montagna@tamucc.edu

Additional Supporting Information may be found in the online version of this article.

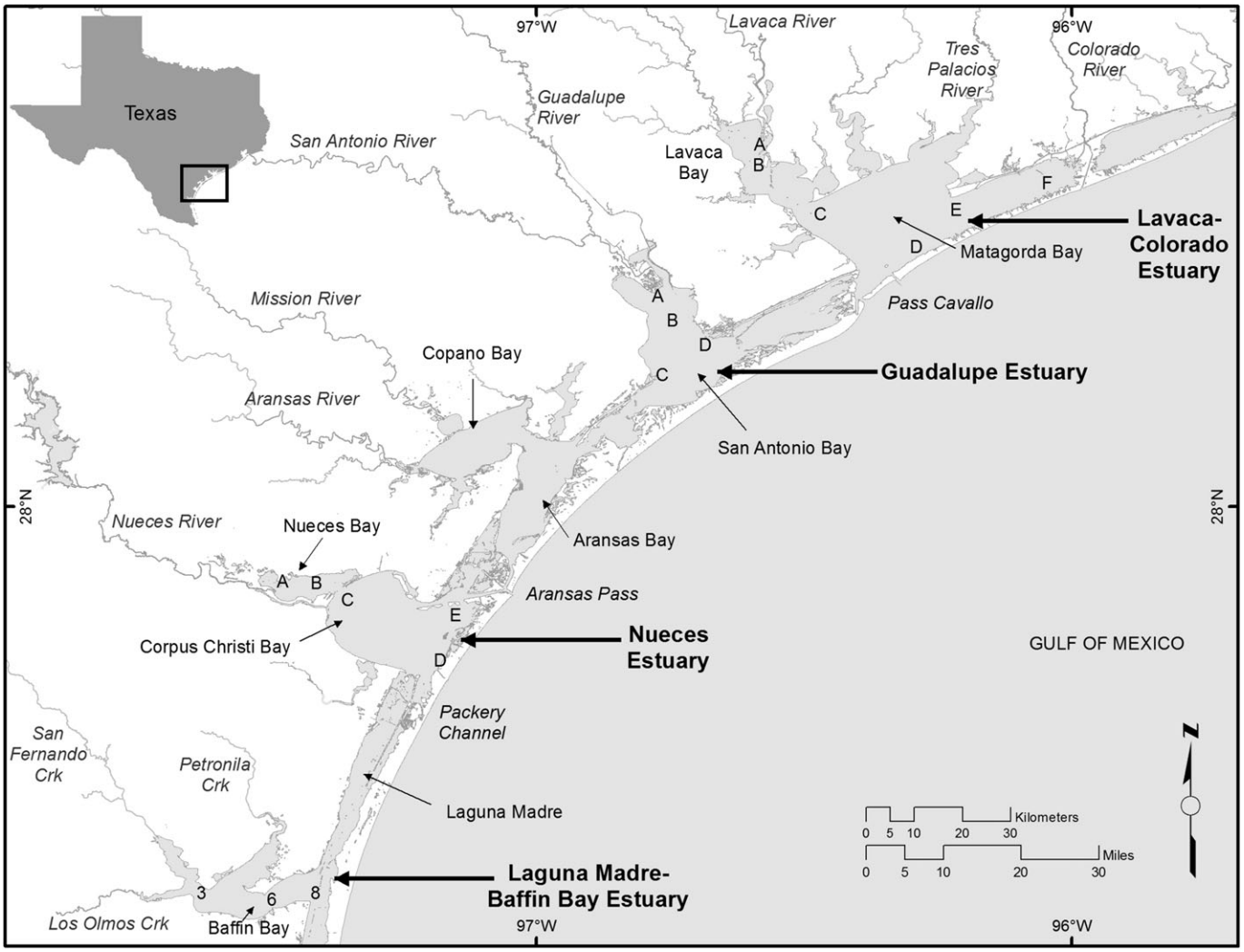

Fig. 1. Map of study area with 18 stations and eight bays within four estuaries along the Texas coast.

Most secondary bays are fed by just one or two rivers draining watersheds. The estuaries are hydrologically diverse because of a climatic gradient of decreasing rainfall and concomitant freshwater inflow from higher to lower latitudes (Longley 1994). Along this gradient, rainfall decreases to the point where inflow balance (i.e., sum of water inputs minus evaporation and diversions) changes from positive to negative. The net effect is a gradient of estuaries with similar physical characteristics but sharp salinity differences.

The study is motivated by a need to determine the role that hydrology plays in the biogeochemistry of estuaries, given dramatic climatic and anthropogenic changes that are affecting river flows to coastal regions worldwide (Olsen et al. 2006; Montagna et al. 2013). The working hypothesis is that on the Texas coast and regions with similar watershed geology, rivers act as a hydrological switch, with river inflow delivering nutrients from land and weathering products from karst aquifers and drainage basins that have carbonate minerals. In terms of nutrient inputs, eutrophication effects such as low dissolved oxygen (DO) may be observed. But during dry periods, the reduced inflow can cause acidification (or dealkalization) effects due to decreased riverine alkalinity input and within estuary alkalinity consumption. The latter was discovered recently and is worth further investigation (Hu et al. 2015). The approach here is to compare negative, neutral, and positive estuaries over time to capture different hydrological regimes and subsequent effects on estuarine biogeochemistry.

Methods

Study area

To test the hypothesis that hydrology drives biogeochemistry, four estuaries were studied: Baffin Bay (BB), Nueces Estuary (NC), Guadalupe Estuary (GE), and Lavaca-Colorado Estuary (LC) (Fig. 1). Although the estuaries share common geomorphological characteristics with one another, they are

Table 1. Characteristics of Texas estuaries from the present study. Estuaries are listed from high to low latitude. Shown are area at mean low tide, average annual rainfall 1951–1980, average annual freshwater inflow balance 1941–2009, and average estuary-wide salinity 1976–2007. Standard deviation in parentheses.

Estuary	Area* (km^2)	Watershed population† (*n*)	Watershed land use† (%Urban/%Ag)	Nitrogen load‡,§ (kg km^{-2} yr^{-1})	Mean residence time‖,¶ (yr)	Rainfall# (cm yr^{-1})	Inflow** (10^6 m^3 yr^{-1})	Salinity†† (psu)
Lavaca-Colorado	1158	1,432,800	4/29.8	123–133	0.21	102	3999 (3420)	19.98 (4.58)
Guadalupe	551	1,590,933	7.2/36.7	361	0.19	91	2799 (2083)	16.81 (4.90)
Nueces	433	424,884	1.9/17.5	52–56	0.46	76	323 (823)	28.99 (3.78)
Baffin Bay-Upper Laguna Madre	1139	75,842	1.3/32.2	145–717	>1	69	–734 (968)	35.94 (7.00)

*Diener (1975).
†Bricker et al. (2007).
‡Alexander et al. (2001).
§Rebich et al. (2011).
‖Longley (1994).
¶Wetz et al. (2017).
#Larkin and Bomar (1983).
**Texas Water Development Board (https://waterdatafortexas.org/coastal/hydrology).
††Montagna et al. (2011).

different in historical hydrology and long-term average salinity (Table 1). Within NC, GE, and LC, there is a positive salinity gradient from secondary bays to primary bays. In contrast, BB is typically a negative estuary where evaporation rates are greater than freshwater runoff into the system, and during drought, salinity may increase from the mouth to upper estuary.

Sample collection

Discrete water samples were collected quarterly between July 2013 and July 2016. Samples were collected within 10 cm of the surface for chlorophyll *a* (Chl *a*), inorganic nutrients, dissolved organic carbon (DOC) and total dissolved nitrogen (TDN), calcium concentration, and carbonate system variables, i.e., pH, total dissolved inorganic carbon (DIC), and total alkalinity (TA). In addition, a multiparameter sonde was used to measure DO, pH, temperature, salinity, and conductivity at each site and time point. Sondes were precalibrated and postcalibrated to ensure quality control of data.

Sample analysis

For determination of chlorophyll concentrations, a known volume of water sample was gently (≤ 5 mm Hg) filtered through Whatman 25 mm GF/F filters that were then stored frozen until analysis. Chl *a* was extracted from the filters by soaking for 18–24 h in either 95% methanol (LC, GE, NC) or 90% High-performance liquid chromatography (HPLC)-grade acetone at –20°C (BB), after which Chl *a* was determined fluorometrically with a Turner Trilogy fluorometer without acidification.

For LC, GE, and NC, inorganic nutrient concentrations [nitrate + nitrite (NO_x), ammonium, orthophosphate, silicate] were determined from the filtrate of water that passed through a 0.45 μm polycarbonate filter and stored frozen (–20°C) until analysis within 2 weeks of collection (Paudel et al. 2015, 2017). Samples were analyzed with an O.I. Analytical Flow Solution IV analyzer. Check standards of known concentrations, as well as matrix spikes and laboratory duplicates were run after every 10 samples. Method detection limits were 0.01 μM for NO_x, 0.03 μM for ammonium, 0.01 μM for orthophosphate, and 0.07 μM for silicate. For BB, inorganic nutrient concentrations were determined from the filtrate of water samples that were passed through 25 mm GF/F filters and stored frozen (–20°C) until analysis (Wetz et al. 2017). After thawing to room temperature, samples were analyzed on a Seal QuAAtro autoanalyzer. Standard curves with five different concentrations were run daily at the beginning of each run. Fresh standards were made prior to each run by diluting a primary standard with low nutrient surface seawater. Deionized water (DIW) was used as a blank, and DIW blanks were run at the beginning and end of each run, as well as after every 8–10 samples to correct for baseline shifts. Method detection limits were 0.02 μM for NO_x and ammonium, and < 0.01 μM for orthophosphate and silicate.

For determination of DOC and TDN concentrations, water samples were collected in acid-washed amber polycarbonate

bottles. Bottles were stored on ice until return to a shore-based facility where processing of samples occurred. DOC and TDN were determined using the filtrate of water samples that passed through precombusted 25 mm GF/F filters and stored frozen (–20°C) until analysis. Samples were subsequently analyzed using the High Temperature Catalytic Oxidation method on a Shimadzu TOC-Vs analyzer with nitrogen module. Standard curves were run twice daily using a DIW blank and five concentrations of either acid potassium phthalate solution or potassium nitrate for DOC and TDN, respectively. Three to five subsamples were taken from each standard and water sample and injected in sequence. Reagent grade glucosamine was used as a laboratory check standard and inserted throughout each run, as were Certified Reference Material Program (CRMP) deep-water standards of known DOC/TDN concentration. Average daily CRMP DOC and TDN concentrations were 45.2 ± 7.0 μmol L^{-1} and 31.8 ± 2.1 μmol L^{-1}, respectively. Dissolved organic nitrogen (DON) was determined by subtracting dissolved inorganic nitrogen (ammonium, NO_x) from TDN.

For carbonate system (TA and total DIC) samples, 250 mL narrow-neck borosilicate glass bottles were used to collect water samples. Hundred microliter of saturated $HgCl_2$ was added to the water sample to stop biological activity and the bottles were sealed with the aid of Apiezon® grease and a rubber band. The samples were stored at 4°C in the dark until analysis, usually within 2–3 weeks of sample collection. Polypropylene bottles (125 mL) were used to collect Ca^{2+} samples. In the study by Bockmon and Dickson (2014), filtration for coastal water carbonate system characterization was recommended. However, no significant difference between filtered and unfiltered samples was found in these samples (Hu et al. 2015), thus unfiltered samples were used exclusively in this study. For DIC analysis, a 0.5 mL water sample was acidified by 0.5 mL 10% H_3PO_4 using a 2.5 mL syringe pump, and the released CO_2 was then analyzed on an AS-C3 DIC analyzer (Apollo SciTech). For TA analysis, 25 mL water sample was titrated with a 0.1 M HCl solution (in 0.5 M NaCl) using an AS-ALK2 alkalinity titrator (Apollo SciTech). Temperature of the titration vessel was maintained at 22 ± 0.1°C using a water-jacketed circulation system. Certificate Reference Material (Dickson et al. 2003) was used to construct the standard curve for the DIC analysis and to calibrate the acid used for TA titration. Both DIC and TA analyses had a precision of ± 0.1%. Two different approaches were taken to measure pH of the water samples. For salinity less than 20 and greater than 40, a high-precision Thermo Orion Ross™ glass electrode calibrated with three pH buffers (4.01, 7.00, and 10.01, Fisher Scientific) was used with a precision of ± 0.01 pH units; for salinity at the range of 20–40, a purified m-cresol purple obtained from Robert Byrne's lab was used following the equation in Liu et al. (2011) to calculate pH on an experimental setup similar to Carter et al. (2013). The spectrophotometric method has a measurement precision of ± 0.0004 pH units. Both pH measurements were done at 25°C.

Ca^{2+} concentration was determined by potentiometric titration (Kanamori and Ikegami 1980) using ethylene glycol tetraacetic acid (EGTA) as the titrant. The end-point was detected using a Metrohm® calcium-selective electrode on a semi-automated titration system. This method had a precision of ± 0.2% or better for estuarine waters.

Carbonate saturation state with respect to aragonite (Ω_{arag}) at in situ conditions was calculated using the program CO2SYS (Pierrot et al. 2006) and lab measured pH and DIC were taken as input variables, and the program derived in situ Ω_{arag} was corrected using titration-obtained Ca^{2+} concentrations. Average propagated error of Ω_{arag} at low salinity (< 20) conditions was estimated to be ± 0.06 and at high salinity (> 20) conditions, ± 0.01. The choice of using DIC-pH as input pair in the CO2SYS calculations was based on the fact that estuarine waters often contain non-negligible amount of non-carbonate alkalinity species (Cai et al. 1998; Hunt et al. 2011; Abril et al. 2015; Nydahl et al. 2017), which would result in bias in the carbonate system speciation calculations.

Statistical analyses

All chemical variables (X) were log transformed using $\ln(X + 1)$, except for pH, which is already on logarithmic scale. Transformation of the values was necessary for the residuals to meet the assumptions of analysis of variance. Additionally, for the principal components analysis (PCA), all variables were standardized to a normal distribution with a mean of 0 and variance of 1 using the PROC STANDARD module contained in the SAS Institute Inc (2013) software suite.

PCA was used to classify the samples based on the standardized data set. The PCA is a variable reduction technique that can be used to reduce a large number of variables to a reduced set of new variables, which are uncorrelated and contain most of the variance in the original data set. PCA was performed using the PROC FACTOR module contained in the SAS software suite. The FACTOR analysis was run using the PCA method on the correlation matrix and the Varimax rotation transformation. Variables that were sums of other variables, such as dissolved inorganic nitrogen (DIN) and Ω_{arag}, were not used in the analysis because the information is in the other variables and they are correlated.

ANOVA was used to identify scales of spatial variability among the samples. Samples were collected from several stations within each primary and secondary bay comprising an estuary. Stations are thus nested within the bays, and the bays are nested within estuaries, so the experimental design is a partially hierarchical, two-way ANOVA that can be described by the following statistical model: $Y_{ijklm} = \mu + \alpha_j + \beta_k + \alpha\beta_{jk} + \gamma_{k(l)} + \delta_{m(kl)} + e_{(i)jklm}$, where Y_{ijklm} is the dependent response variable, μ is the overall sample mean, α_j is the main fixed effect for sampling date where j = 1 to 13; β_k is the main fixed effect for estuary where k = 1 to 4 for either BB, NC, GE, or LC; $\alpha\beta_{jk}$ is the main fixed effect for the interaction between dates and estuaries, $\gamma_{k(l)}$ is the main effect for primary and

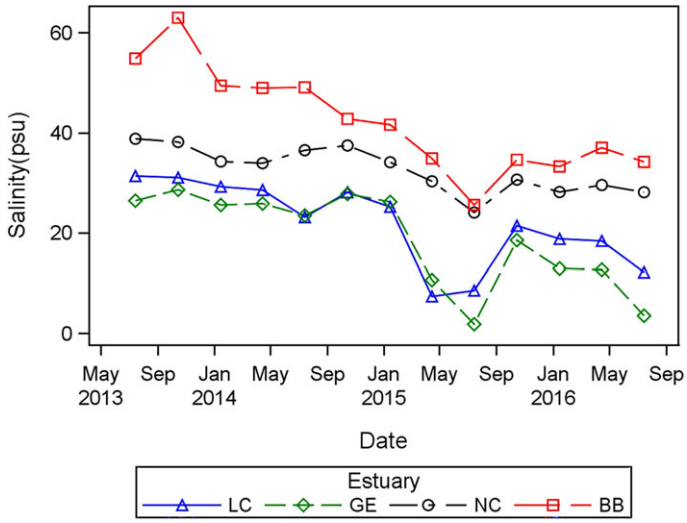

Fig. 2. Average salinity in each estuary over all sampling periods. Abbreviations: BB, Baffin Bay; GE, Guadalupe Estuary; LC, Lavaca-Colorado Estuary; NC, Nueces Estuary.

secondary bays that are nested (or unique) to the estuaries and are thus a random effect as denoted by the parentheses around the subscript *l* that represents the eight bays (Lower BB, Upper BB, Corpus Christi Bay [CCB], Nueces Bay, Lower San Antonio Bay, Upper San Antonio Bay, Matagorda Bay, and Lavaca Bay) all of which are nested unique to one of the four estuaries; $\delta_{m(kl)}$ is the term for the specific 18 stations within bays, thus stations are completely nested within estuaries and bays; and $e_{(i)jklm}$ is the random error term for each of the *i* measurements within cells. This model was computed using PROC GLM in SAS Institute Inc (2013), and because this is a mixed model the expected mean squares (EMS), variance components, and correct *F*-tests were also computed. The *F*-test for dates, bays, and stations is formed by dividing the EMS for the main effects by the mean square error. The *F*-test for the date × estuary interaction is formed by dividing the EMS of the main effect by the EMS of the station effect. The *F*-test for the estuary main effect is formed by dividing the EMS of the main effect by the EMS of the sum of the date × estuary interaction and the station effect.

Results

The salinity gradient among estuaries followed the hydrological gradient along the coast. For example, the estuary receiving the least freshwater inflow (BB) always had the highest salinities, while NC always had an intermediate salinity, and GE and LC had the lowest salinities (Fig. 2; Table 2). There was a distinct dry period from July 2013 to February 2015, followed by a wet period from February 2015 onward. The temporal pattern in salinity reflected these precipitation/hydrological shifts for each estuary (Fig. 2).

The first principal component (PC1) explained 29% of the variability in the data set, and the second (PC2) explained 20%, for a total of 49% of the variability. PC1 had Ca^{2+} and salinity that were inversely correlated with NO_x, orthophosphate, silicate, pH, and chlorophyll (Fig. 3). Thus, PC1 represents a freshwater inflow index (FwII) because when flow rates are high, salinity is low and nutrient concentrations are high.

Table 2. Mean and standard deviations (in parentheses) for all chemical variables measured during the current study by estuary.

Variable (units)	BB	NC	GE	LC
Temperature (°C)	23.35 (5.35)	23.58 (6.41)	23.40 (7.26)	23.34 (7.06)
Salinity	41.21 (10.42)	32.81 (4.97)	18.76 (10.12)	22.65 (8.69)
DO (mg L^{-1})	5.98 (1.34)	7.44 (1.02)	9.17 (3.34)	8.26 (2.57)
pH	8.20 (0.13)	8.11 (0.13)	8.30 (0.34)	8.20 (0.21)
Secchi (m)	0.54 (0.19)	1.00 (0.56)	0.56 (0.29)	0.77 (0.46)
PO_4 (μmol L^{-1})	0.24 (0.18)	0.97 (1.54)	2.05 (3.11)	1.13 (1.21)
SiO_4 (μmol L^{-1})	65.16 (32.06)	52.04 (38.09)	102.51 (73.86)	47.09 (36.63)
NH_4 (μmol L^{-1})	3.53 (3.10)	1.02 (1.67)	1.15 (1.55)	1.08 (1.34)
NO_x (μmol L^{-1})	0.60 (0.96)	1.14 (1.81)	8.64 (26.49)	4.35 (11.07)
Chl (μg L^{-1})	16.96 (10.61)	7.52 (4.53)	19.29 (15.06)	8.99 (6.54)
TDN (μmol L^{-1})	67.22 (12.30)	30.54 (9.71)	36.44 (32.24)	31.21 (19.66)
DIN (μmol L^{-1})	4.13 (3.68)	2.21 (3.32)	9.80 (26.76)	5.46 (12.02)
DON (μmol L^{-1})	61.56 (15.83)	28.33 (8.83)	26.48 (11.00)	25.76 (11.57)
DOC (μmol L^{-1})	822.72 (136.63)	360.47 (111.43)	382.35 (115.80)	377.67 (147.48)
DIC (μmol L^{-1})	2498.33 (334.94)	2217.69 (140.82)	2621.18 (377.37)	2105.21 (263.30)
TA (μmol kg^{-1})	3132.74 (570.84)	2559.30 (188.02)	2975.94 (365.18)	2356.45 (322.83)
Ca^{2+} (mmol kg^{-1})	11.29 (2.34)	9.77 (1.37)	5.98 (2.63)	6.76 (2.41)
Ω_{arag}	4.98 (1.36)	4.14 (1.22)	5.44 (2.53)	3.35 (1.52)

BB, Baffin Bay; GE, Guadalupe Estuary; LC, Lavaca-Colorado Estuary; NC, Nueces Estuary.

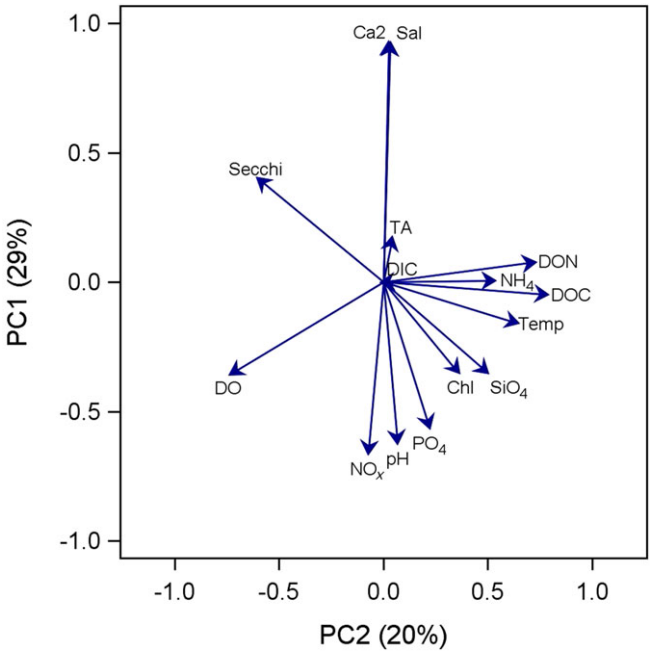

Fig. 3. Principal components (PC) of water quality variable loads. Abbreviations: Ca2, calcium^{+2}; Chl, chlorophyll *a*; DIC, dissolved inorganic carbon; DO, dissolved oxygen; DOC, dissolved organic carbon; DON, dissolved organic nitrogen; NH_4, ammonium; NO_x, nitrite + nitrate; PO_4, phosphate; Sal, salinity; Secchi, Secchi disk depth; SiO_4, silicate; TA, total alkalinity; Temp, temperature.

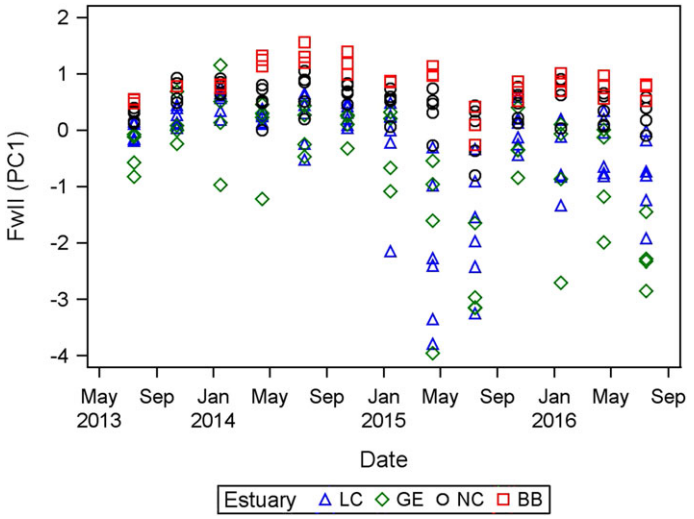

Fig. 4. FwII (i.e., first principal component [PC1]) of chemical variable sample scores for every station-sampling date combination. Abbreviations as in Fig. 2.

PC2 had DOC, DON, ammonium, and temperature that were inversely related to DO and Secchi depth. Thus, PC2 represents a metabolic process because when temperatures are high, dissolved organic matter and ammonia are produced, DO solubility decreases, and DO is consumed at a higher rate under higher temperature. In addition, DO also showed inverse correlation with the FwII, indicative of lower salinity water having higher DO solubility. BB samples have the highest PC1 scores followed by NC, and GE and LC samples have the lowest PC1 scores, indicating freshwater inflow has the greatest effects on GE and LC (Fig. 4). During the dry period, prior to February 2015, there are only a few low PC1 scores, whereas most low PC1 scores occurred during the wet period after February 2015.

There were significant differences among estuaries for salinity, DO, ammonium, DOC, DON, DIC, TA, and Ca^{2+} (Tables 2, 3). There were within estuary differences between primary and secondary bays for all variables except ammonium, NO_x, and DIN. There were station differences within estuary-bays for salinity, pH, phosphate, silicate, NO_x, TDN, DIN, DOC, DON, TA, and Ω_{arag}, but not for temperature, DO, Secchi depth, ammonium, chlorophyll, DIC, and Ca^{2+} (Table 3). Except for temperature, pH, and silicate, most of the variability in water quality constituents was due to estuary differences (Table 3). Temperature, which varies seasonally, had 96% of its variation explained by sampling date. Other variables that had at least 24% of their variability explained by temperature included DO, Secchi depth, orthophosphate, silicate, NO_x, and DIN. Overall, the average variance explained by estuary was 54%, date was 21%, bay was 16%, and station was 3%. Thus, variance components increased with spatial scale, and spatial variability was responsible for 73% of all variability on average.

Across these different estuaries, phosphate (Fig. 5) and DO (Supporting Information Fig. S1) decrease linearly with increasing bay salinity. In contrast, NO_x (Fig. 5), silicate (Supporting Information Fig. S2), and DIN (Supporting Information Fig. S3) exhibit a nonlinear pattern that points to a sink in the intermediate salinity bays. Both DIC and TA exhibit a multiple river end-member mixing scenario, with higher DIC and TA levels observed in Upper San Antonio Bay than in Lavaca Bay (Fig. 6), indicating that freshwater sources have different levels of weathering products. However, from the neutral and the negative estuaries (Nueces-Corpus Christi and BB), DIC and TA exhibited a combination of estuarine mixing and evaporation signals, i.e., DIC, TA, and salinity were all elevated and the latter exceeded seawater salinity during the dry period (Fig. 6). A unique aspect of the chemical constituents observed along the climatic gradient is that some have "U-shaped" mixing curves, where they initially decline, and then increase as salinity increases. This is for DIC and TA (Fig. 6), TDN (Supporting Information Fig. S4), and chlorophyll (Fig. 7). One final pattern that was observed is relatively low concentrations of DOC and DON in the positive and neutral estuaries, and very high concentrations in the negative estuary (Fig. 8).

Discussion

This study encompassed a period of low rainfall, followed by period of much higher rainfall that coincided with a strong

Table 3. Results of ANOVA for each variable. (A) Probability (*p*) values for null hypothesis in the mixed ANOVA. (B) Variance components analysis.

A)	*p* values for mixed ANOVA		
Variable	**Estuary**	**Bay (Est)**	**Station (Est Bay)**
Temperature	0.51	0.01	0.10
Salinity	0.03	0.00	0.03
DO	0.03	0.00	0.25
pH	0.52	0.00	0.00
Secchi	0.31	<0.01	0.63
PO_4	0.33	0.02	<0.01
SiO_4	0.50	0.00	0.01
NH_4	0.00	0.20	0.47
NO_x	0.15	0.34	<0.01
Chl	0.17	<0.01	0.54
TDN	0.12	0.02	<0.01
DIN	0.24	0.42	<0.01
DON	0.05	0.00	0.00
DOC	0.05	0.00	<0.01
DIC	0.03	0.01	0.07
TA	0.02	0.00	0.05
Ca^{2+}	0.02	0.00	0.07
Omega	0.16	0.00	0.04

B)	Variance components (percent)					
Variable	**Date**	**Estuary**	**Date * Est**	**Bay (Est)**	**Station (Est * Bay)**	**MS (error)**
Temperature	96	1	2	1	0	0
Salinity	19	67	3	9	1	1
DO	30	60	2	8	1	0
pH	21	31	6	36	4	1
Secchi	25	43	3	27	1	1
PO_4	28	37	5	25	5	1
SiO_4	28	28	9	31	3	1
NH_4	9	74	10	3	2	2
NO_x	24	42	6	15	11	2
Chl	12	58	4	23	1	1
TDN	6	67	2	20	4	1
DIN	25	30	12	16	14	3
DON	4	78	1	15	2	0
DOC	5	78	2	14	1	0
DIC	3	77	7	10	1	1
TA	4	78	6	10	1	1
Ca^{2+}	17	72	2	8	1	0
Omega	20	51	7	20	2	1
Average	*21*	*54*	*5*	*16*	*3*	*1*

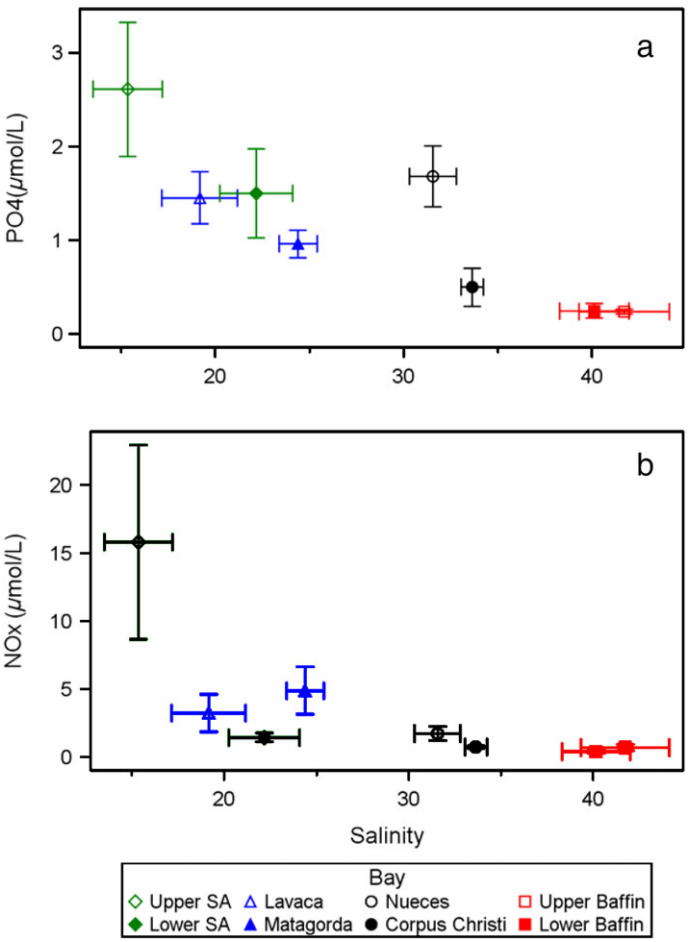

Fig. 5. Relationship between inorganic nutrients mean concentrations and mean salinity by bay. (**a**) Phosphate (PO_4) and (**b**) nitrate + nitrite ($NO_3 + NO_2$) NO_x.

El Niño, which tends to facilitate higher precipitation along the western Gulf of Mexico (Tolan 2007). Each of the estuaries in this study experienced a decrease in salinity as a result of the higher precipitation and subsequent freshwater inflow. Results from this study highlight the important role that freshwater inflow plays in determining estuarine biogeochemistry. Our key findings indicate that carbonate chemistry, nutrients (inorganic and organic), and chlorophyll are not only affected by temporal variability in freshwater inflow within particular estuaries, but also by broad spatial-scale differences in freshwater inflow between estuaries that likely integrate effects over much longer time scales. Carbonate species, nutrients, and chlorophyll are integral components of the estuarine ecosystem in that they determine suitability of a system for shell-forming organisms (e.g., carbonate chemistry), support primary production at the base of the estuarine food web (e.g., nutrients), and provide an indicator of phytoplankton biomass (e.g., chlorophyll). Given ongoing and projected changes in freshwater inflow worldwide due to climatic and anthropogenic changes (Wentz et al. 2007; Durack et al. 2012), it is imperative to understand how the spatial-temporal distribution of estuarine biogeochemical variables can be affected by freshwater inflow variability,

Concentrations of DIC and TA, and pH levels, the major parameters of the carbonate system, were higher during high precipitation/inflow conditions, i.e., after February 2015, and these variables were positively correlated with freshwater inflow in all estuaries except Lavaca-Colorado. We attribute this positive correlation with inflow to the increased input of weathering products from the three rivers, Nueces, San Antonio, and Guadalupe, all originating from the Edward Aquifer that is of karst nature (Woodruff and Abbott 1979). Consequently, the input of this highly buffered river water led to increased pH and Ω_{arag} in the estuaries. An exception to this

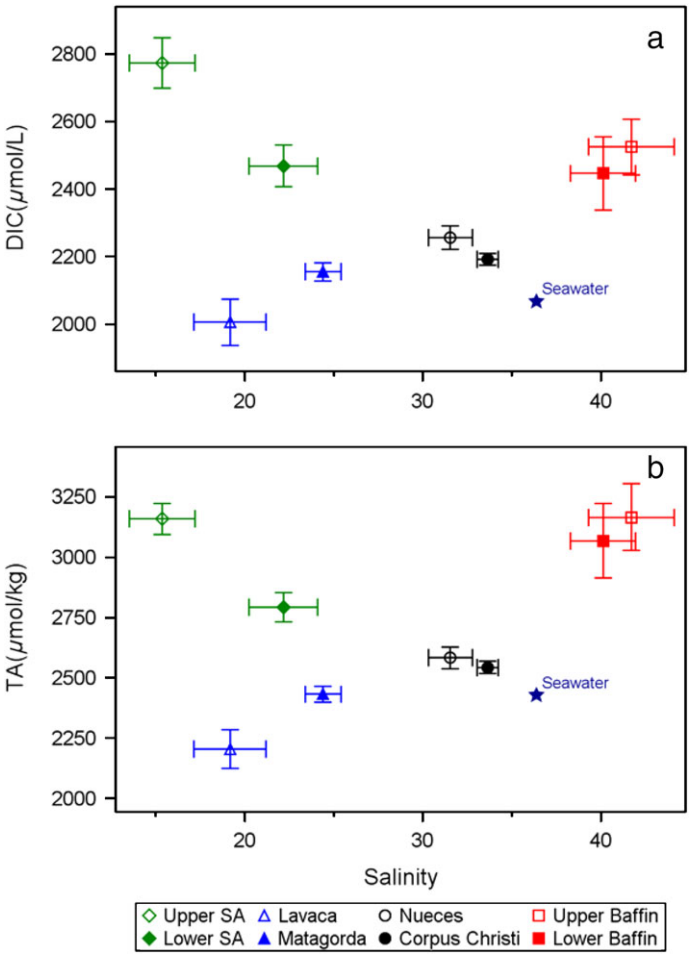

Fig. 6. Relationship between mean concentrations of inorganic carbon and mean salinity by bay, with a seawater reference. (**a**) DIC and (**b**) TA.

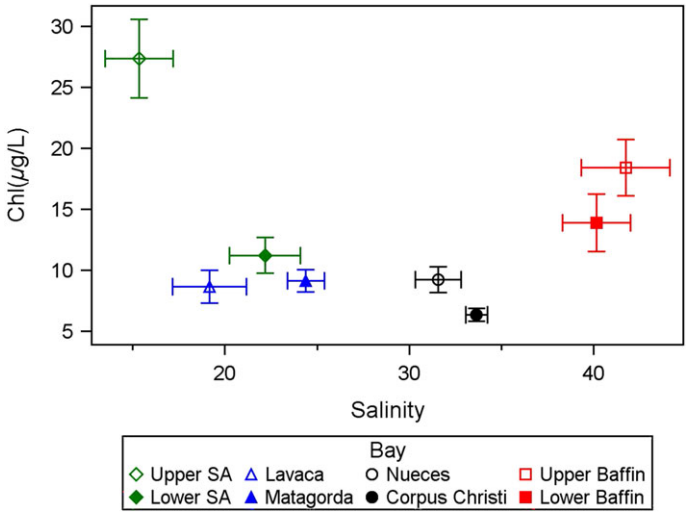

Fig. 7. Relationship between mean chlorophyll (Chl) concentrations and mean salinity by bay.

overall trend of greater buffering of the estuary with higher freshwater inflow is Lavaca-Colorado Estuary. This system actually saw a decrease in DIC, TA, and pH with higher freshwater inflow, owing to lower levels of weathering products in river waters during high inflow seasons. Subsequently, brief but undersaturated conditions were observed in April 2015 and July 2015, with Ω_{arag} as low as 0.06, despite the overall high saturation state during our entire study period (Table 2). Decreases in DIC/TA in Lavaca and Colorado rivers mostly reflected a dilution signal, similar to that in large river systems (Cai et al. 2008). In fact, located in the same physiographic region as the Colorado River that contributes to LC, Brazos River has limited carbonate dissolution along its drainage basin despite the middle Brazos flowing through limestone bedrock (Zeng et al. 2011). Thus conceptually, higher freshwater inflow to Guadalupe, Nueces, and BB should lead to increased buffering capacity, whereas in Lavaca-Colorado the opposite occurred, with potential negative impacts on shell-forming organisms in the system (Salisbury et al. 2008; Mathis et al. 2011). This finding highlights the important role that both watershed mineralogy and freshwater inflow play as drivers of estuarine carbonate chemistry (Yao and Hu 2017).

On average, inorganic nutrient concentrations tended to be highest in upper San Antonio Bay, followed by Lavaca-Colorado, Nueces, and BB. While this pattern roughly follows that of annual freshwater inflow magnitude, there is an important exception. Specifically, the average annual inflow to the Lavaca-Colorado system is higher than to San Antonio Bay, yet inorganic nutrient concentrations were lower in Lavaca-Colorado. One possible explanation for this is that watershed land use activity exerted a larger control on inorganic nutrient loadings to the estuaries (via influence on river inorganic nutrient concentrations) than did the magnitude of the freshwater inflow. In support of this, we note that the average inorganic nutrient concentration of each estuary was more closely proportional to the percentage of urbanized land in the watersheds than to the magnitude of freshwater inflow. Urbanization has been shown to correlate with inorganic nutrient content of rivers and streams (Bowen and Valiela 2001; Kaushal et al. 2008; Rothenberger et al. 2009). Furthermore, data collected from July 2013 to July 2016 by a state water quality monitoring program is supportive of this idea. That data shows that NO_x concentrations in the San Antonio River were eightfold to 32-fold higher than in the Lavaca or Colorado Rivers, and total phosphorus concentrations were threefold to fourfold higher (Wetz unpubl. data).

Given the established pattern of inorganic nitrogen concentrations across estuaries, it was expected that chlorophyll concentration would be higher in San Antonio Bay, and would become progressively lower in Lavaca-Colorado, Nueces, and BB. Indeed, this trend was observed for Lavaca-Colorado, Guadalupe, and Nueces estuaries, indicating a significant influence of river-derived inorganic nutrients on phytoplankton growth in these systems. However, this relationship did not hold true in BB. In fact, chlorophyll was very high in this

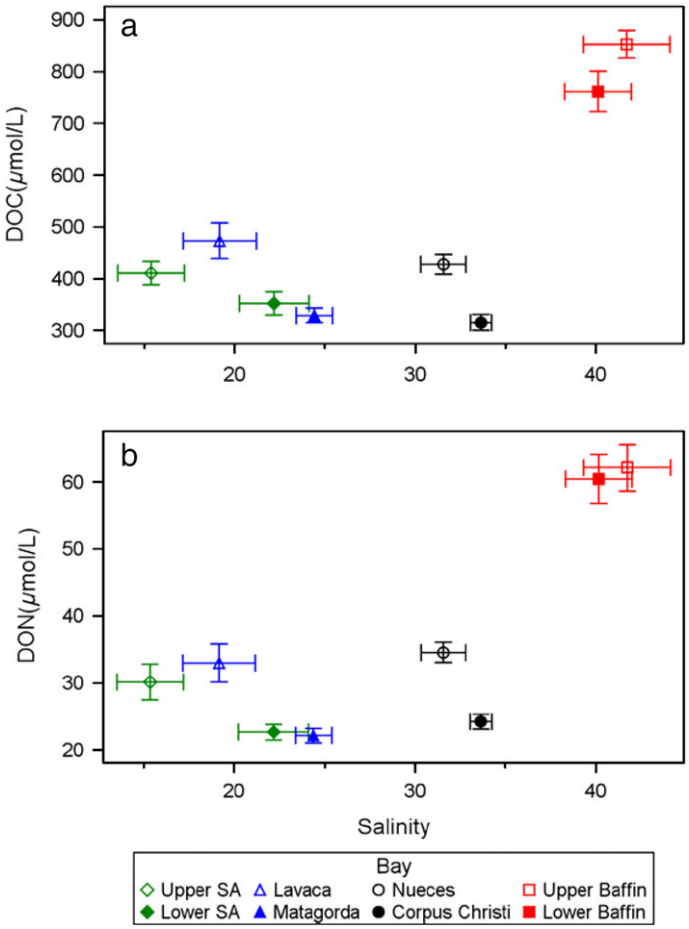

Fig. 8. Relationship between mean dissolved organic nutrient concentrations and mean salinity by bay. (**a**) DOC and (**b**) DON.

system despite its much lower inorganic nutrient concentrations (Table 2). Wetz et al. (2017) suggested that this was possible because of the potential for very high rates of nitrogen recycling and retention, as well as high concentrations of DON that may be used by mixotrophic phytoplankton in the system. This finding further exemplifies the importance of not only watershed land use activity but also circulation on estuarine nutrient-phytoplankton dynamics. BB receives relatively little freshwater input except during episodic high rainfall periods (Wetz et al. 2017). Yet the system displays a number of symptoms of eutrophication including high and increasing chlorophyll and nitrogen concentrations (Wetz et al. 2017). Although inorganic nutrient concentrations are low in the system, DON concentrations are over twofold higher in BB than the other estuaries, and TDN is quite high relative to the other systems as well (Table 2). Anecdotal evidence points to the main external sources of nitrogen as likely being input of crop residue from the watershed and/or input of algal decay products from the fertilizer and wastewater-enriched streams of the BB watershed (Wetz et al. 2017). In terms of circulation, Wetz et al. (2017) suggested that the very long residence time (on average, > 1 yr) of BB allows for effective uptake and recycling of nutrients, a phenomenon that is common to long residence time systems (Cloern 2001; Pinckney et al. 2001). Indeed, An and Gardner (2002) found evidence of high potential rates of dissimilatory nitrate reduction to ammonium at the sediment-water interface in BB, leading to high potential rates of ammonium flux to the water column. As will be discussed later, evaporation is responsible for only a small fraction of the organic matter enrichment in BB.

The importance of freshwater inflow variability becomes more apparent when comparing short-term dynamics rather than long-term dynamics. For example, the concentrations of the major inorganic nutrient species (NO_x, phosphate, silicate) were higher in all four estuaries during high precipitation/inflow conditions. This is consistent with the study of Mooney and McClelland (2012) from the nearby Copano Bay, which showed ephemeral high inorganic nutrient concentrations following episodic rain events. Even in BB, higher frequency (i.e., biweekly to monthly) sampling indicates that it is not uncommon to see ephemeral very high inorganic nutrient concentrations following rain events (Wetz et al. unpubl. data). One exception to this trend of higher nutrients during high rainfall periods is silicate in BB, which was generally lower during the higher precipitation period. The reason for this is unclear, although lower than expected silicate has been attributed to enhanced biological (by diatoms) uptake or input from low-mineral content, organic-rich watersheds in other systems (Balls 1994).

It was expected that we would see a gradient of DOC and POC concentrations that align with the magnitude of freshwater inflow to each estuary due to allochthonous inputs. This pattern did not materialize however. POC concentrations largely mirrored those of chlorophyll, thus we suspect that the overall pattern that emerged for POC is reflective of patterns in the phytoplankton community. DOC concentrations were similar between the Guadalupe, Lavaca-Colorado, and Nueces Estuaries, but much higher in BB (cf. DON, Table 2). Explanations for the DOC enrichment in BB are bound to be similar as for DON enrichment described above. However, this still leaves unexplained why DOC concentrations in the other three estuaries did not align with the magnitude of freshwater inflow or salinity. One possibility is that the riverine endmember DOC concentration was lower for Lavaca-Colorado and Guadalupe estuaries than Nueces. Salinity-DOC relationships extrapolated to zero salinity suggest that this is a possibility, as the estimated zero salinity DOC concentrations were 874 μM for NC during the wet period, 682 μM for Lavaca-Colorado, and 453 μM for GE (Supporting Information Fig. S5). The Nueces estimate is tenuous, however, as we do not have data from salinity < 20, thus, there is considerable uncertainty as to the actual DOC concentration as one approaches the mouth of its main river. Another possibility is that the DOC in Lavaca-Colorado and GE is simply more labile than DOC in the NC and is more rapidly removed from the system, hence

concentrations are lower than expected in those estuaries. Both Lavaca-Colorado and Guadalupe Estuaries have a relatively high proportion of agricultural and/or urbanized land use in their watershed. Previous work has shown that DOC derived from these land use types tends to be much more labile than from relatively undisturbed watersheds (Servais et al. 1987; Petrone et al. 2009). Although not complete at the time of this manuscript, a companion study is currently examining amino acid composition of the organic matter in rivers of each estuary to characterize its lability (cf. Dauwe et al. 1999).

DO is a key water quality variable that integrates the effects of many biogeochemical processes. During this study, on average, DO was highest in the high inflow/low salinity GE, and became progressively lower from Lavaca-Colorado to Nueces to BB. This gradient could be attributed to a combination of effects arising from salinity and biological gradients. In terms of salinity, it is well known that oxygen solubility decreases as salinity increases (Weiss 1970), and our results are one of the first to demonstrate these effects on a near coast-wide scale. Specifically, results highlight the important role that freshwater inflow and subsequent salinity changes can play in terms of dictating oxygen levels in estuaries. It is possible that microbial dynamics played a role as well. For instance, the higher phytoplankton biomass (as denoted by chlorophyll) in GE may have contributed to the higher oxygen levels, whereas high organic carbon concentrations and dominance of the phytoplankton community by mixotrophic phytoplankton may have contributed to high respiration rates that lowered oxygen levels in BB. Work is ongoing to understand the role of salinity vs. microbial dynamics in terms of influences on oxygen in several of these systems.

In traditional estuarine studies on solute distribution and dynamics, evaporation is usually not accounted for. The primary reason is that estuaries usually have relatively short residence times so that evaporation is not a significant term in changing concentrations of dissolved constituents. However, residence time in many lagoonal estuaries along the northwestern Gulf of Mexico are significantly longer compared to river-dominated estuaries (Solis and Powell 1999). Furthermore, in this subtropical region, relatively high evaporation rates are common, ranging from $\sim 117 \pm 14$ cm yr^{-1} on the upper Texas coast to 158 ± 15 cm yr^{-1} on the lower Texas coast (http://www.twdb.texas.gov/surfacewater/conditions/evaporation/). Precipitation minus evaporation generates a slightly positive freshwater balance ($\sim 10 \pm 32$ cm yr^{-1}) on the upper Texas coast, but a large negative value ($\sim -91 \pm 25$ cm yr^{-1}) on the lower Texas coast. Given the shallowness of these estuaries (2–3 m) and the decreasing river inflow moving south along the coast, a succession from river-estuarine mixing scenario to evaporation-dominated scenario may be possible as a controlling factor on solute distributions.

In an estuarine setting, river and ocean water mixing typically exhibits a linear relationship between a solute concentration and salinity if there is no reaction that significantly alters the solute, and the intercept at 0 salinity would represent the freshwater end-member. We took TA = 2428 μmol kg^{-1} at salinity 36.4 (Hu et al. 2015) as the ocean end-member, then we used the two secondary bays (Upper San Antonio and Lavaca) as the "composite" river end-member and let them mix with the coastal seawater. The calculated *y*-intercepts indicate that average river TA as 3691 μmol kg^{-1} and 1958 μmol kg^{-1} for Guadalupe and Lavaca rivers, respectively. We did not collect river water end-member during our sampling period. However, Guadalupe and Lavaca Rivers have long-term average TA of 4168 ± 667 μmol kg^{-1} and 2628 ± 1208 μmol kg^{-1}, respectively, based on the data set collected by Texas Commission on Environmental Quality (1969–2010). Both predicted TA values at zero salinity appeared to be lower than actual river values. In comparison, the predicted TA for the Nueces River was 3600 μmol kg^{-1}, which was higher than the long-term Nueces River TA of 3152 ± 389 μmol kg^{-1}. Therefore, as water residence time increases to the south, relative contributions of evaporation vs. reaction must also change.

A schematic graph was used to identify the relative contributions of evaporation vs. reaction in the distribution of solute, using TA as an example (Fig. 9). In the two upper coast estuaries, lower predicted TA (*y*-intercepts, TA' in Fig. 9) than river TA indicates TA consumption within an estuary. This coincides with the fact that the upper coast estuaries have more abundant benthic calcifiers (Pollack et al. 2011), and calcification removes TA from the water column (the lower dashed line in Fig. 9). In comparison, Nueces Bay water had elevated predicted TA (compared to river TA) that indicates the importance of evaporation in controlling solute distribution (upper dashed line in Fig. 9; also see Hu et al. 2015). This latitudinal shift of river TA vs. the mixing *y*-intercept suggests that evaporation plays a more important role in estuarine carbonate species with decreasing latitude on the Texas coast. A hydrologically extreme condition was observed in BB. Because the tidal inlets that lead to Laguna Madre are small and freshwater sources are relatively inconsequential, the only major water source that contributes to BB would come through CCB. If the average TA of both upper and lower BB (3165 μmol kg^{-1} and 3068 μmol kg^{-1}) at salinity 41.72 and 40.13, respectively is normalized to average CCB salinity 33.64, then the TA would be 2552 μmol kg^{-1} and 2572 μmol kg^{-1}. In comparison, average measured TA in CCB was 2543.6 ± 24.6 μmol kg^{-1} during our entire sampling period, which is similar to the "diluted" BB water. Similarly, if we take average Ca^{2+} concentrations from upper and lower BB (12.02 mmol kg^{-1} and 11.81 mmol kg^{-1}) and normalize to CCB salinity, the calculated Ca^{2+} (9.69 mmol kg^{-1} and 9.90 mmol kg^{-1} in upper and lower BB, respectively) also agreed well with average CCB Ca^{2+} concentration (9.92 ± 0.16 mmol kg^{-1}). Therefore, based on TA and Ca^{2+} data, water in BB can be considered as "concentrated" CCB water for the inorganic solutes.

Following the same reasoning, if both DOC and DON in CCB water are assumed to be concentrated as the water moved

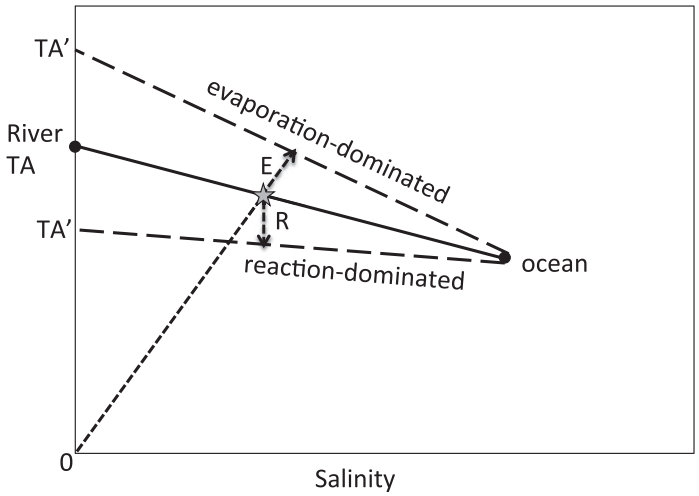

Fig. 9. Schematic illustration of the effects of evaporation vs. reaction on estuarine solute distribution. "E" represents evaporation of estuarine water and "R" represents reactions that consume the solute. TA' represents apparent river end-member based on ocean end-member and altered estuarine signals.

into BB, then the concentrating effect would have increased DOC concentration from 316 μM in CCB to 391 μM and 376 μM in upper and lower BB, respectively, and increased DON concentration from 24.2 μM to 30.0 μM and 28.9 μM in upper and lower BB, respectively. However, DOC and DON concentrations in both upper and lower BB far exceeded what would be expected due to evaporation, as the evaporation only scenario would produce DOC and DON at 45–50% of observed concentrations. In other words, concentration increase due to evaporation alone only accounted for 8–9% of total DOC and DON inventories in BB. Therefore, as discussed above, eutrophication must have led to the large enrichment of DOC and DON in BB.

Conclusions

By comparing geomorphologically similar estuaries that differ primarily in their freshwater inflow balance, this study has led to emerging paradigms related to the influence of hydrology on estuarine biogeochemical functioning. For example, evidence points to the importance of "new" nitrogen inputs from rivers as a driver of productivity in positive estuaries, whereas recycled or organic-based nitrogen inputs are of primary importance in negative estuaries. These broad differences in nutrient conditions between systems may be a key driver of differences in phytoplankton community composition. Specifically, phytoplankton composition in the negative estuary in this study (BB) tends to be dominated by mixotrophic flagellates (e.g., *Aureoumbra lagunensis*, "brown tide") and dinoflagellates (Wetz unpubl. data), whereas the river-dominated estuaries of the upper Texas coast tend to have diatoms and flagellates that are capable of fast growth and utilization of riverine nitrate (Ornolfsdottir et al. 2004; Roelke et al. 2017). The implications are significant because many mixotrophic phytoplankton, including *A. lagunensis*, are harmful to the environment and can have negative implications for fisheries (Burkholder et al. 2008; Gobler and Sunda 2012). Although demonstrated here in subtropical estuaries, it is likely that the finding of increased harmful algal bloom risk due to long residence time and prevalence of reduced nutrients are applicable to other estuarine systems facing reduced freshwater inflow now and in the future. In the future, we aim to further explore linkages between inflow conditions, nutrient quantity/quality and phytoplankton composition in these estuaries. In terms of carbonate chemistry, positive estuaries that receive river input originating from a karst aquifer, will buffer coastal waters under "average" freshwater inflow conditions. However, Lavaca-Colorado, despite having a drainage basin that includes limestones, exhibited a dilution effect during high inflow period. This dilution effect led to carbonate undersaturation and decreases in pH similar to rivers in temperate and subarctic regions. Surprisingly, the lack of freshwater inflow alone did not lead to "acidified" conditions in the negative estuary, as evaporation concentrated the dissolved species and increased buffer in this system, and water column production also enhanced the buffer.

On a global scale, estuarine systems are expected to experience changes in the timing and magnitude of freshwater inflows due to climate change and increasing human consumptive demands. Many regions will become hotter and drier, which will reduce drainage from watersheds and increase evaporation so that the net effect is reduced freshwater inflow to estuaries. As human populations in the coastal regions continue to increase, the demand for more freshwater will further reduce environmental flows in rivers, streams, and to estuaries, while also increasing nutrient runoff in the absence of mitigation activities (Wetz and Yoskowitz 2013). The implications of the findings for subtropical lagoons in the current study are that these two forces (i.e., climate and population changes) may combine to have a multiplicative effect on the hydrology of estuaries, which in conjunction with changes to land use will drive biogeochemical conditions of estuarine waters in other types of estuaries. These kinds of changes could cause regime shifts in many types of estuaries as they become more sluggish and more saline.

References

Abril, G., and others. 2015. Technical Note: Large overestimation of pCO_2 calculated from pH and alkalinity in acidic, organic-rich freshwaters. Biogeosciences **12**: 67–78. doi: 10.5194/bg-12-67-2015

Alexander, R. B., R. A. Smith, G. E. Schwarz, S. D. Preston, J. W. Brakebill, R. Srinivasan, and P. A. Pacheco. 2001. Atmospheric nitrogen flux from the watersheds of major estuaries

of the United States: an application of the SPARROW watershed model. *In* R. A. Valigura, R. B. Alexander, M. S. Castro, T. P. Meyers, H. W. Paerl, P. E. Stacey, and R. E. Turner [eds.], Nitrogen loading in coastal water bodies: an atmospheric perspective. Pp. 119–170.

An, S., and W. Gardner. 2002. Dissimilatory nitrate reduction to ammonium (DNRA) as a nitrogen link, versus denitrification as a sink in a shallow estuary (Laguna Madre/Baffin Bay, Texas). Mar. Ecol. Prog. Ser. **237**: 41–50. doi:10.3354/meps237041

Balls, P. W. 1994. Nutrient inputs to estuaries from 9 Scottish east coast rivers - influence of estuarine processes on inputs to the North Sea. Estuar. Coast. Shelf Sci. **39**: 329–352. doi:10.1006/ecss.1994.1068

Bricker, S., B. Longstaff, W. Dennison, A. Jones, K. Boicourt, C. Wicks, and J. Woerner. 2007. Effects of nutrient enrichment in the nation's estuaries: a decade of change. NOAA Coastal Ocean Program Analysis Series No. 26, National Centers for Coastal Ocean Science Silver Spring, MD 328 pp.

Bockmon, E. E., and A. G. Dickson. 2014. A seawater filtration method suitable for total dissolved inorganic carbon and pH analysis. Limnol. Oceanogr.: Methods **12**: 191–195. doi:10.4319/lom.2014.12.191

Bowen, J. L., and I. Valiela. 2001. The ecological effects of urbanization of coastal watersheds: Historical increases in nitrogen loads and eutrophication of Waquoit Bay estuaries. Can. J. Fish. Aquat. Sci. **58**: 1489–1500. doi:10.1139/cjfas-58-8-1489

Burkholder, J. M., P. M. Glibert, and H. M. Skelton. 2008. Mixotrophy, a major mode of nutrition for harmful algal species in eutrophic waters. Harmful Algae **8**: 77–93. doi:10.1016/j.hal.2008.08.010

Cai, W.-J., W. Yongchen, and R. E. Hodson. 1998. Acid-base properties of dissolved organic matter in the estuarine waters of Georgia, USA. Geochim. Costmochim. Acta **62**: 473–483. doi:10.1016/S0016-7037(97)00363-3

Cai, W.-J., and others. 2008. A comparative overview of weathering intensity and HCO_3^- flux in the world's major rivers with emphasis on the Changjiang, Huanghe, Zhujiang (Pearl) and Mississippi Rivers. Cont. Shelf Res. **28**: 1538–1549. doi:10.1016/j.csr.2007.10.014

Carter, B. R., J. A. Radich, H. L. Doyle, and A. G. Dickson. 2013. An automatic system for spectrophotometric seawater pH measurements. Limnol. Oceanogr.: Methods **11**: 16–27. doi:10.4319/lom.2013.11.16

Cloern, J. E. 2001. Our evolving conceptual model of the coastal eutrophication problem. Mar. Ecol. Prog. Ser. **210**: 223–253. doi:10.3354/meps210223

Dauwe, B., J. J. Middelburg, P. M. J. Herman, and C. H. R. Heip. 1999. Linking diagenetic alteration of amino acids and bulk organic matter reactivity. Limnol. Oceanogr. **44**: 1809–1814. doi:10.4319/lo.1999.44.7.1809

Dickson, A. G., J. D. Afghan, and G. C. Anderson. 2003. Reference materials for oceanic CO_2 analysis: A method for the certification of total alkalinity. Mar. Chem. **80**: 185–197. doi:10.1016/S0304-4203(02)00133-0

Diener, R. A. 1975. Cooperative Gulf of Mexico estuarine inventory and study- Texas area description, p. 129. U.S. Department of Commerce, NOAA technical report, National Marine Fisheries Service Circular 393; [accessed 2018 June 13]. Available from http://spo.nmfs.noaa.gov/Circulars/CIRC393.pdf

Durack, P. J., S. E. Wijffels, and R. J. Mater. 2012. Ocean salinities reveal strong global water cycle intensification during 1950 to 2000. Science **336**: 455–458. doi:10.1126/science.1212222

Gobler, C. J., and W. G. Sunda. 2012. Ecosystem disruptive algal blooms of the brown tide species, *Aureococcus anophagefferens* and *Aureoumbra lagunensis*. Harmful Algae **14**: 36–45. doi:10.1016/j.hal.2011.10.013

Hu, X., J. Beseres Pollack, M. R. Mccutcheon, P. A. Montagna, and Z. Ouyang. 2015. Long-term alkalinity decrease and acidification of estuaries in Northwestern Gulf of Mexico. Environ. Sci. Technol. **49**: 3401–3409. doi:10.1021/es505945p

Hunt, C. W., J. E. Salisbury, and D. Vandemark. 2011. Contribution of non-carbonate anions to river alkalinity and overestimation of pCO_2. Biogeosciences **8**: 5159–3076. doi:10.5194/bgd-8-5159-2011

Kanamori, S., and H. Ikegami. 1980. Computer-processed potentiometric titration for the determination of calcium and magnesium in seawater. J. Oceanogr. **36**: 177–184. doi:10.1007/BF02070330

Kaushal, S. S., and others. 2008. Interaction between urbanization and climate variability amplifies watershed nitrate export in Maryland. Environ. Sci. Technol. **42**: 5872–5878. doi:10.1021/es800264f

Larkin, T. J., and G. W. Bomar. 1983. Climatic atlas of Texas. Texas Department of Water Resources; [accessed 2018 June 13]. Available from http://www.twdb.texas.gov/publications/reports/limited_printing/doc/LP192.pdf

Liu, X., M. C. Patsavas, and R. H. Byrne. 2011. Purification and characterization of meta-cresol purple for spectrophotometric seawater pH measurements. Environ. Sci. Technol. **45**: 4862–4868. doi:10.1021/es200665d

Longley, W. L. [ed.]. 1994. Freshwater inflows to Texas bays and estuaries: Ecological relationships and methods for determination of needs. Texas Water Development Board and Texas Parks and Wildlife Department, Austin, Texas [accessed 2018 June 13]. Available from https://repositories.lib.utexas.edu/handle/2152/6728

Mathis, J. T., J. N. Cross, and N. R. Bates. 2011. The role of ocean acidification in systemic carbonate mineral suppression in the Bering Sea. Geophys. Res. Lett. **38**: L19602. doi:10.1029/2011GL048884

Montagna, P. A., J. Brenner, J. Gibeaut, and S. Morehead. 2011. Coastal impacts, p. 96–123. *In* J. Schmandt, G. R. North, and J. Clarkson [eds.], The impact of global warming on Texas, 2nd ed. Univ. of Texas Press.

Montagna, P. A., T. A. Palmer, and J. B. Pollack. 2013. Hydrological changes and estuarine dynamics (Springerbriefs in environmental sciences). Springer.

Mooney, R. F., and J. W. McClelland. 2012. Watershed export events and ecosystem responses in the Mission-Aransas National Estuarine Research Reserve, South Texas. Estuaries Coast. **35**: 1468–1485. doi:10.1007/s12237-012-9537-4

Nydahl, A. C., M. B. Wallin, and G. A. Weyhenmeyer. 2017. No long-term trends in pCO_2 despite increasing organic carbon concentrations in boreal lakes, streams, and rivers. Global Biogeochem. Cycles **31**: 985–995. doi:10.1002/2016GB005539

Olsen, S. B., T. V. Padma, and B. D. Richter. 2006. Managing freshwater inflows to estuaries: A methods guide, p. 44. U.S. Agency for International Development, Washington, D.C. [accessed 2017 August 11]. Available from http://pdf.usaid.gov/pdf_docs/pnadh650.pdf

Ornolfsdottir, E. B., S. E. Lumsden, and J. L. Pinckney. 2004. Nutrient pulsing as a regulator of phytoplankton abundance and community composition in Galveston Bay, Texas. J. Exp. Mar. Bio. Ecol. **303**: 197–220. doi:10.1016/j.jembe.2003.11.016

Paudel, B., P. A. Montagna, and L. Adams. 2015. Variations in the release of silicate and orthophosphate along a salinity gradient: Do sediment composition and physical forcing have roles? Estuar. Coast. Shelf Sci. **157**: 42–50. doi:10.1016/j.ecss.2015.02.011

Paudel, B., P. A. Montagna, M. Besonen, and L. Adams. 2017. Inorganic nitrogen release from sediment slurry of riverine and estuarine ecosystems located at different river regimes. Mar. Freshw. Res. **68**: 1282–1291. doi:10.1071/MF16260

Petrone, K. C., J. S. Richards, and P. F. Grierson. 2009. Bioavailability and composition of dissolved organic carbon and nitrogen in a near coastal catchment of south-western Australia. Biogeochemistry **92**: 27–40. doi:10.1007/s10533-008-9238-z

Pierrot, D., E. Lewis, and D. W. R. Wallace. 2006. MS Excel Program developed for CO_2 system calculations. ORNL/CDIAC-105a. Carbon Dioxide Information Analysis Center, Oak Ridge National Laboratory, U.S. Department of Energy, Oak Ridge, Tennessee.

Pinckney, J. L., H. W. Paerl, P. Tester, and T. L. Richardson. 2001. The role of nutrient loading and eutrophication in estuarine ecology. Environ. Health Perspect. **109**: 699–706. doi:10.1289/ehp.01109s5699

Pollack, J. B., H.-C. Kim, E. K. Morgan, and P. A. Montagna. 2011. Role of flood disturbance in natural oyster (*Crassostrea virginica*) population maintenance in an estuary in South Texas, USA. Estuaries Coast. **34**: 187–197. doi:10.1007/s12237-010-9338-6

Potter, I. C., B. M. Chuwen, S. D. Hoeksema, and M. Elliott. 2010. The concept of an estuary: A definition that incorporates systems which can become closed to the ocean and hypersaline. Estuar. Coast. Shelf Sci. **87**: 497–500. doi:10.1016/j.ecss.2010.01.021

Pritchard, D. W. 1952. Estuarine hydrography, p. 243–280. *In* H. E. Landsberg [ed.], Advances in geophysics, v. I. Academic Press.

Pritchard, D. W. 1967. What is an estuary: Physical viewpoint, p. 52–63. *In* G. H. Lauff [ed.], Estuaries. American Association for the Advancement of Science.

Rebich, R. A., N. A. Houston, S. V Mize, D. K. Pearson, P. B. Ging, and C.E. Hornig. 2011. Sources and delivery of nutrients to the northwestern Gulf of Mexico from streams in the south-central United States. Journal of the American Water Resources Association **47**: 1061–1086

Roelke, D. L., H. P. Li, C. J. Miller-DeBoer, G. M. Gable, and S. E. Davis. 2017. Regional shifts in phytoplankton succession and primary productivity in the San Antonio Bay System (USA) in response to diminished freshwater inflows. Mar. Freshw. Res. **68**: 131–145. doi:10.1071/MF15223

Rothenberger, M. B., J. M. Burkholder, and C. Brownie. 2009. Long-term effects of changing land use practices on surface water quality in a coastal river and lagoonal estuary. Environ. Manag. **44**: 505–523. doi:10.1007/s00267-009-9330-8

Salisbury, J., M. Green, C. Hunt, and J. Campbell. 2008. Coastal acidification by rivers: A threat to shellfish? Eos Trans. AGU **89**: 513–514. doi:10.1029/2008EO500001

SAS Institute Inc. 2013. SAS/STAT® 13.1 User's Guide. SAS Institute Inc.

Servais, P., G. Billen, and M. C. Hascoet. 1987. Determination of the biodegradable fraction of dissolved organic matter in waters. Water Res. **21**: 445–450. doi:10.1016/0043-1354(87)90192-8

Solis, R. S., and G. L. Powell. 1999. Hydrography, mixing characteristics, and residence times of Gulf of Mexico estuaries, p. 29–61. *In* T. S. Bianchi, J. R. Pennock, and R. R. Twilley [eds.], Biogeochemistry of Gulf of Mexico estuaries. John Wiley & Sons.

Tolan, J. M. 2007. El Niño-Southern Oscillation impacts translated to the watershed scale: Estuarine salinity patterns along the Texas Gulf Coast, 1982 to 2004. Estuar. Coast. Shelf Sci. **72**: 247–260. doi:10.1016/j.ecss.2006.10.018

Turner, R. E. 2001. Of manatees, mangroves, and the Mississippi River: Is there an estuarine signature for the Gulf of Mexico? Estuaries **24**: 139–150. doi:10.2307/1352940

Weiss, R. F. 1970. The solubility of nitrogen, oxygen and argon in water and seawater. Deep-Sea Res. Oceanogr. Abstr. **17**: 721–735. doi:10.1016/0011-7471(70)90037-9

Wentz, F. J., L. Ricciarduli, K. Hilburn, and C. Mears. 2007. How much more rain will global warming bring? Science **317**: 233–235. doi:10.1126/science.1140746

Wetz, M. S., and D. W. Yoskowitz. 2013. An "extreme" future for estuaries? Effects of extreme climatic events on estuarine water quality and ecology. Mar. Pollut. Bull. **69**: 7–18. doi:10.1016/j.marpolbul.2013.01.020

Wetz, M. S., E. K. Cira, B. Sterba-Boatwright, P. A. Montagna, T. A. Palmer, and K. C. Hayes. 2017. Exceptionally high

organic nitrogen concentrations in a semi-arid South Texas estuary susceptible to brown tide blooms. Estuar. Coast. Shelf Sci. **188**: 27–37. doi:10.1016/j.ecss.2017.02.001

Woodruff, C. M., and P. L. Abbott. 1979. Drainage-basin evolution and aquifer development in a karstic limestone terrain South-Central Texas, U.S.A. Earth Surf. Process. Landf. **4**: 319–334. doi:10.1002/esp.3290040403

Yao, H., and X. Hu. 2017. Responses of carbonate system and CO_2 flux to extended drought and intense flooding in a semiarid subtropical estuary. Limnol. Oceanogr. **62**: S112–S130. doi:10.1002/lno.10646

Zeng, F.-W., C. Masiello, and W. Hockaday. 2011. Controls on the origin and cycling of riverine dissolved inorganic carbon in the Brazos River, Texas. Biogeochemistry **104**: 275–291. doi:10.1007/s10533-010-9501-y

Acknowledgments

We thank the dedicated citizen scientist volunteers who were integral in the Baffin Bay data collections. We also thank the following individuals for assistance with field collections and sample processing: Leslie Adams, Noe Barrera, Victor Batres, Kalman Bugica, Kelsey Fisher, Anne-Marie Gavlas, Kenneth Hayes, Larry Hyde, Rick Kalke, Melissa McCutcheon, Elani Morgan, Jessica Tolan, Cory Staryk, Sarah Tominack, Lily Walker, Hongming Yao, Hongjie Wang, and many more. This work was supported in part by grants from the Coastal Bend Bays and Estuaries Program; the Texas Water Development Board 1448311638 and 1600011924; the National Oceanic and Atmospheric Administration grant NA15NOS4780185; an Institutional Grant (award NA14OAR4170102) to the Texas Sea Grant College Program from the National Sea Grant Office; the Texas Coastal Management Program Grant pursuant to National Oceanic and Atmospheric Administration award NA14NOS4190139; the Celanese Corporation; Kleberg County; the Coastal Conservation Association; and the Saltwater Fisheries Enhancement Association. All views, opinions, findings, conclusions, and recommendations expressed in this material are those of the author(s) and do not necessarily reflect the opinions of the Texas Sea Grant College Program, the National Oceanic and Atmospheric Administration or any of its subagencies.

Conflict of Interest

None declared.

Submitted 09 October 2017
Revised 06 April 2018
Accepted 18 May 2018

Associate editor: Josette Garnier